PHILOSOPHICAL TRANSACTIONS OF THE ROYAL SOCIETY A MATHEMATICAL, PHYSICAL & ENGINEERING SCIENCES

Physical Processes in the Benthic Boundary Layer

K. J. Richards

Phil. Trans. R. Soc. Lond. A 1990 **331**, 3-13
doi: 10.1098/rsta.1990.0052

Phil. Trans. R. Soc. Lond. A **331**, 3–13 (1990)

Printed in Great Britain

Physical processes in the benthic boundary layer

By K. J. Richards

Department of Oceanography, The University, Southampton SO9 5NH, U.K.

The benthic, or bottom, boundary layer is the region of the ocean adjacent to the ocean floor. Bottom-generated turbulence mixes properties such as temperature and salinity to produce a homogeneous layer a few tens of metres thick. The physical structure of the layer affects biological, chemical and geological processes at or near the ocean floor and how these processes communicate with the ocean interior. Recent observations have uncovered a richness in structure of the layer; benthic fronts, benthic storms, fluid ejection and enhanced mixing behind sea-mounts. Results from observational and modelling studies is reviewed. The implications for the dispersion of tracers and residence time within the layer is discussed.

1. Introduction

To the casual observer, the region of the oceans waters close to the bottom, ten or so metres thick, may seem insignificant when considering the flow, chemistry or biology of the much deeper ocean above. However, it is here that chemical species are exchanged across the sediment–water interface, benthic communities live and sediment is transported by currents frequently producing bed forms, changing the morphology of the surface and thus shaping the currents that formed the bed features. Bottom friction is considered to be an important sink of energy of motions in the ocean interior through Ekman pumping. This Ekman pumping, through vortex stretching, also affects the synoptic-scale eddy field above (see §3.3). A knowledge of the physical processes controlling the flow and density structure close to the ocean floor is vital to understanding the chemical, biological and sedimentalogical processes at or near the ocean floor and their relations with the ocean interior.

Close to the ocean floor currents are retarded by bottom friction. The resultant vertical shear of the flow becomes turbulent. The turbulence mixes properties such as temperature and salinity to produce a homogeneous layer some tens of metres thick. The layer is often capped by a region of strong density gradient inhibiting exchange of properties between the mixed layer and above. Turbulence generated at the bottom is restricted to this layer, the benthic boundary layer. Until recently observations of the benthic boundary layer have been limited. Measurements of temperature and salinity showed a mixed layer often several times that expected by existing one-dimensional models (see, for example, Armi & Millard 1976). We have since realized that the simplistic one-dimensional view of the layer is inappropriate. Even over a flat ocean floor the layer is horizontally inhomogeneous. Armi & D'Asaro (1980) studied the bottom mixed layer at a site in the western Atlantic and found the height of the mixed layer to vary between 5 and 60 m over horizontal distances of 20 km and periods of 15 days. The layer is at least intermittently turbulent (D'Asaro 1982) with the turbulence being confined to the mixed layer. The much weaker stratification of the eastern Atlantic (Saunders 1983) and eastern Pacific (Hayes 1979) makes it difficult to detect the presence of a mixed layer. However, by careful analysis of temperature measurements made in the eastern Atlantic it has

been possible to deduce that the average height of the layer is approximately 50 m, becoming less than 10 m on some occasions and greater than 100 m on others (Saunders & Richards 1985). Measurements using electromagnetic current meters show the flow to be turbulent with the ratio of the variance of the flow to the mean to be similar to other geophysical boundary layers (Elliott 1984). The observations of Saunders (1983) show that the height of the mixed layer is not correlated with the strength of the flow above the layer as is implied in a one-dimensional model. Even in strong current régimes, such as that studied in high-energy benthic boundary layer events (HEBBLE), much of the changes in structure of the boundary layer at a given point are believed to be due to advection (Weatherly & Kelly 1985; Gross & Nowell 1990, this symposium).

As mentioned above, the relatively strong density gradient at the top of the mixed layer inhibits exchange of fluid and chemical constituents with the ocean interior. There are, however, a number of processes that can cause fluid to escape from the benthic boundary layer. A study of these processes is important in assessing the role of the layer in isopycnal mixing processes in the ocean and the flux of tracers from the ocean floor to the interior. It is only through such processes that the interior can communicate with the sea-bed. A number of these escape processes will be discussed in §3. The bulk of the discussion will centre on the action of synoptic-scale eddies. Dispersion of a tracer is investigated and an estimate given of the residence time for particles to remain within the mixed layer. But first, we will consider the vertical structure of the benthic boundary layer.

2. Vertical structure

The current close to the sea-bed has three main components, the semi-diurnal tide, inertial oscillations and low frequency synoptic-scale eddies. On the Madeira abyssal plain, for example, these have periods of 12.4 h, 22 h and 50 to 100 days and amplitudes 3 cm s^{-1}, 1.3 cm s^{-1} and 2.5 cm s^{-1} respectively (Saunders 1983). The development time of the mixed layer is of order a few days. We can therefore ignore the time variation of the synoptic-scale eddies in studying the vertical structure of the layer. The unsteadiness of the flow at tidal and inertial frequencies, however, does have to be taken into account.

For a horizontally homogeneous flow over a flat surface the height of the boundary layer will depend on the Earth's rotation, the distribution of density and the unsteadiness of the flow. As has already been mentioned, observations suggest that the height must be controlled by other factors, such as horizontal advection. However, a study of the one-dimensional case is instructive in giving the expected vertical distribution of mean flow and turbulent stresses within the layer, the surface stress and the development time of the layer.

A number of authors have considered the one-dimensional problem (Wimbush & Munk 1970; Weatherly & Martin 1978; Bird *et al.* 1982; Richards 1982*a*). The heat flux is taken to be zero (the flux of heat due to geothermal heating has been shown to be negligible (Wimbush & Munk 1970)). Models differ in the turbulent closure taken. Richards (1982*a*) uses a second-order closure scheme based on that used by Wyngaard (1975) for a stably stratified atmospheric boundary layer. The prime reason for going to a second-order scheme was to include time history effects on the turbulence (so called rapid distortion effects). The results for a typical case are shown in figure 1. This shows the development after 3 days of an initially linear temperature gradient with buoyancy frequency $N = 10^{-3}$ s^{-1} under the action of a steady

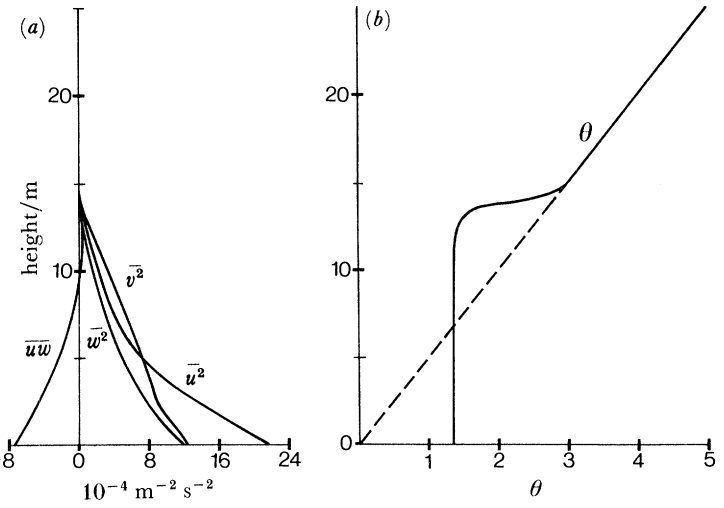

FIGURE 1. Profiles of the turbulent stress components $\overline{uw}$, the variance components $\overline{u^2}$, $\overline{v^2}$, and $\overline{w^2}$ and the mean (non-dimensional) temperature θ for a stably stratified steady flow of 5 cm s^{-1} with buoyancy frequency $N = 10^{-3}$ s^{-1} after three days of mixing (Richards 1982*a*).

current of $U_0 = 5$ cm s^{-1}. The Coriolis parameter $f = 10^{-4}$ s^{-1}. A mixed layer of 13 m has developed, which is capped by a region of strong density gradient. The height of the profiles of Reynolds stresses are restricted to this layer. The friction velocity $u_* = 4.38 \times 10^{-2} U_0$. The direction of the flow veers with height on a height scale of $0.8u_*/f$ with the angle of the surface flow to the geostrophic flow above being 13.2°. As the layer thickens the density gradient strengthens and inhibits further mixing.

The results suggest that the maximum height of the mixed layer for a steady current U_0, is given approximately by

$$h_0 = 0.1 U_0 (f/N)^{\frac{1}{2}}/f. \tag{1}$$

The growth of the layer after this height predicted by the model is very small (due to diffusion of turbulent energy). It is also after this height that internal waves effectively radiate away energy that was formerly available for increasing the layer depth. The height given by (1) is approximately twice that given by Weatherly & Martin (1978) who, using a criterion based on the local Richardson number, find

$$h_0 = 0.05 U_0/f(1 + (N^2/f^2))^{\frac{1}{4}}. \tag{2}$$

The final stages of development of the model of Richards (1982*a*) are very dependent on the modelling of third-order correlation terms in the Reynolds stress equations. Expressions (1) and (2) should therefore be treated as upper and lower bounds, respectively, on the height of the mixed layer.

The time development of the mixed layer height is given approximately by

$$h = h_0(1 - e^{-at}), \tag{3}$$

where $a^{-1} \approx 3$ days. This is approximately twice the development time given by the model of Weatherly & Martin (1978). The reason for this difference is the inclusion of rapid distortion effects in the turbulence model of Richards (1982*a*) so that local shear and stress terms are no longer exactly in phase and the production of turbulent kinetic energy is reduced.

For an unsteady flow the depth of the mixed layer depends on the frequency of the flow, ω.

PHILOSOPHICAL TRANSACTIONS OF THE ROYAL SOCIETY A MATHEMATICAL, PHYSICAL & ENGINEERING SCIENCES

For $\omega > 1.5f$ the equilibrium height of the layer is less than that for the steady case. For a semi-diurnal tide with $\omega = 2f$ the height is 25% less than the steady case. For inertial oscillations ($\omega = f$) the unstratified boundary layer is essentially unbounded. The time derivative term balances the Coriolis term away from the surface in the horizontal momentum equation. In practice the flow is stratified and the depth of the layer will be limited by the radiation of inertial and internal waves as in (1).

3. Horizontal structure: escapes from the mixed layer

A number of processes occurring at or close to the bottom that can affect the horizontal structure of the benthic boundary layer are sketched in figure 2. As suggested in the sketches these processes can also lead to an escape of boundary fluid together with associated tracers, etc. The various processes are discussed in the following sections.

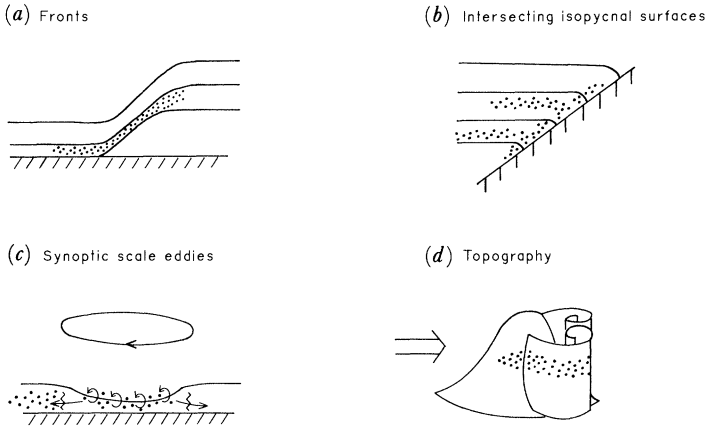

Figure 2. Sketches of a number of processes that can develop horizontal structure in the benthic boundary layer and that can cause boundary fluid to escape from the bottom. The solid lines represent isopycnal surfaces and the dotted regions a tracer.

3.1. *Fronts*

A striking feature of the temperature records in the benthic boundary layer is the presence of frontal features. Thorpe (1983) describes persistent fronts of about 4 m °C which are advected with the tidal flow. A typical front has a width of 300 m and a tilt of 10° to the horizontal. One front was observed to extend over 30 km in the horizontal and 600 m in the vertical. Possible mechanisms for the formation of these fronts include surface convergences caused by synoptic scale motions similar to frontal formation in the upper ocean (McVean & Woods 1980) or the direct action of eddies as outlined in §3.3.2.

The ejection of fluid close to the bottom is possible along the isopycnal surfaces. This process has been observed in the upper ocean (Woods *et al.* 1977). There are no direct observations in the deep ocean.

3.2. *Sloping boundaries and intersecting isopycnal surfaces*

A sloping boundary will intersect the isopycnal surfaces in the ocean. This can also occur on a flat surface if the isopycnals themselves are sloping. Fluid originally in the mixed layer can then escape along a surface of the same density. The processes occurring at sloping boundaries

will be discussed in detail by Thorpe *et al.* (1990, this symposium). Here the process is illustrated by the results from a hydrographic station taken on the Madeira Rise (a slope of 10^{-2}), figure 3. Profiles of potential temperature and transmittance are shown. The potential temperature shows a mixed layer 50 m thick with a weak temperature gradient above. The changes in transmittance are due to changes in sediment content, the lower the signal the higher the concentration of particulate matter. The mixed layer is characterized by low values indicating active mixing. Above the mixed layer a series of layers extending to 300 m above the bottom can be seen. These layers will have originated further up the slope where the relevant isopycnal surface intersects. As the fluid moves away from the actively mixed bottom layer suspended particules will settle with the concentration falling off with distance from the surface. These layers are often referred to as nephloid layers. At 700 m above the bottom a very distinct nephloid layer is seen.

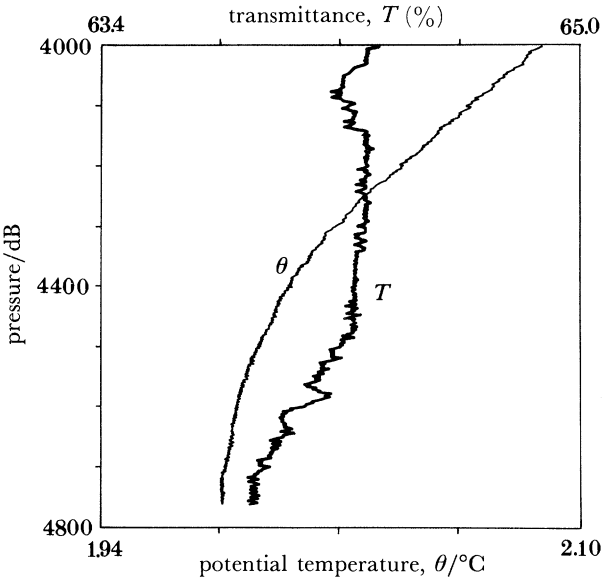

FIGURE 3. Potential temperature, θ, and transmittance, T, profiles close to the bottom from a CTD station taken on the Madeira Rise, *Discovery* cruise 139 (Elliott *et al.* 1983).

3.3. *Synoptic-scale eddies*

3.3.1. *Variation of mixed layer height*

Horizontal variations in the interior flow of the ocean will cause deformations of the height of the bottom mixed layer through Ekman pumping. A major contribution to the horizontal variation in currents in the deep ocean is from synoptic-scale eddies with horizontal length scales of 50–200 km and speeds of a few centimetres per second. Armi & D'Asaro (1980) suggest that the variations in mixed layer structure they observed are due to the action of synoptic-scale eddies. Direct observation of the interaction of eddies and the mixed layer is difficult due to both observational difficulties at such depths and a decoupling between the forcing agent, the eddies, and the layer structure (Richards 1984).

Ekman pumping causes a divergence of fluid within the mixed layer and hence reduction in the height of the layer under anticyclonic eddies and a convergence and thickening under cyclonic eddies.

Arguments based on the conservation of potential vorticity show that a relatively small distortion of the mixed layer height ($O(10\text{ m})$) will induce an $O(1)$ change in the vorticity of a synoptic-scale eddy in contact with the bottom. A model to study the synoptic-scale forcing of the benthic boundary layer needs to be coupled with a model of the ocean interior. Such a model has been developed by Richards (1984). The interaction of eddies and the bottom mixed layer can have interesting consequences for the system as a whole. Due to frictional effects the advection speed of disturbances in the mixed layer differs from that in the interior. This can induce an instability (Richards 1982*b*) or generate strong zonal flows (Richards 1984).

A typical result from the model of Richards (1984) is shown in figure 4. The parameters of the experiment are similar to experiment 8 of Richards (1984) but taken on an f plane ($\beta = 0$) to give a homogeneous, isotropic turbulence field. The flow is considered in an open box 500 km square, which is assumed to be periodic in both horizontal directions. In the vertical the

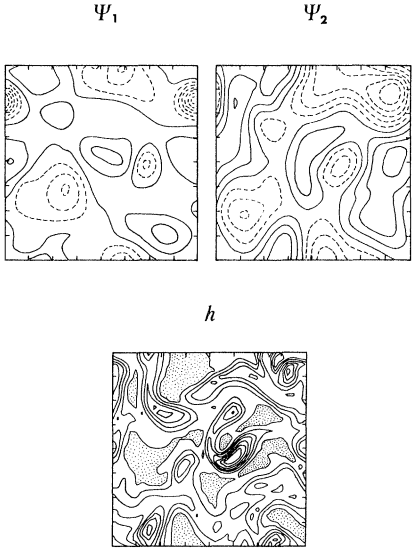

FIGURE 4. Typical streamfunction maps for the flow in the upper two layers Ψ_1, Ψ_2 and the mixed layer height, h, from the model of Richards (1984). The box is 500 km square. The average speed of the flow in the upper two layers is 4 cm s^{-1}. The contour interval for h is 12 m. The shaded regions are where h has been depressed below its equilibrium height.

model has three layers, the upper two model the stratified interior of the ocean. Their depths H_1, H_2 and densities ρ_1, ρ_2 are chosen so that the barotropic and first baroclinic modes of the model are similar to those of the ocean. The lowest layer is the bottom mixed layer. The mixed layer height is assumed restricted by stratification and capped by a strong density gradient. The flow is governed by the quasi-geostrophic potential vorticity equation in the upper two layers. A constant eddy viscosity is used in the boundary layer equations so that an explicit equation can be derived for the mixed layer height. Energy is input into the upper layer to produce an eddy field. These eddies interact with the second layer, which in turn interacts with the mixed layer where the energy is dissipated (see Richards (1984) for details). Figure 4 shows the instantaneous streamfunction fields for the upper two layers and the mixed layer height. The undisturbed mixed layer height is taken to be 30 m. Those regions below this height are shaded in the figure.

The eddies in the second layer have an average speed of 4 cm s^{-1} and have a length scale of

50 km (the horizontal length scale is taken to be the zero crossing of the transverse velocity correlation). The mixed layer height has small intense features with regions of large gradient. The height of the mixed layer varies between 0 and 100 m and has a horizontal scale of 35 km. Changes in mixed layer height are found to be dominated by horizontal advection. Although the vorticity of the eddies is responsible for creating deformations of the mixed layer height the two quickly become decorrelated.

3.3.2. *Entrainment and mixed layer detachment*

When the thickness of the mixed layer is reduced by the action of eddies the top of the mixed layer is brought closer to the bottom. The turbulent energy at the interface between the mixed layer and interior increases and fluid is entrained into the mixed layer from above producing a patch of boundary layer fluid that is lighter than its surroundings (figure 2*c*). Entrainment may also occur in a manner suggested by Smeed (1987). In a laboratory experiment he produced anticyclonic motion in a deep layer of fluid above a thin dense layer. The interface is depressed. Lighter interior fluid is swept under the heavier boundary layer fluid by the Ekman flux. A convective instability then takes place producing mixing between the two fluids.

In either case the warm patch of fluid may be lifted off the bottom by buoyancy forces. The observations of Armi & D'Asaro (1980) show the existence of interior layers uniform in temperature above the bottom mixed layer. There is evidence to suggest that these interior layers are formed by the detachment of the bottom mixed layer and may be the principal mechanism for fluid to escape the bottom layer. Measurements of heat fluxes suggest that the exchange time (the time for fluid to enter, mix and leave the bottom layer) is between 4 and 600 days (Armi & D'Asaro 1980). From their measurements of detached mixed layers Armi & D'Asaro estimate the exchange time to be roughly 100 days.

The residence time for fluid to remain within the bottom layer therefore depends on the length of time it takes a fluid particle to come into contact with a warm patch (see §3.3.3).

Entrainment–detrainment processes have to be necessarily parametrized in the model of Richards (1984). The evolution of the temperature field of the mixed layer in the model shows areas of warmer water which are surrounded by regions of strong temperature gradients, these are very persistent, lasting well over 100 days. At a fixed location the height of the mixed layer is found to vary over a period of approximately 20 days with occasional sharp increases in temperature occurring (figure 5). Episodes of similar structure and duration are seen in the temperature records of Armi & D'Asaro (1980). It is possible that the fronts observed by

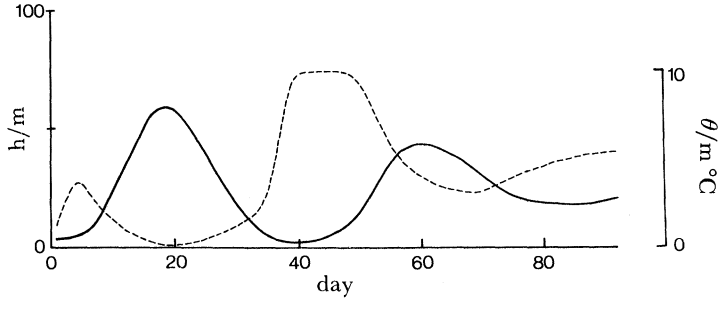

FIGURE 5. The height (solid line) and temperature (dashed line) of the model mixed layer at a fixed point as a function of time.

Thorpe (1983) could also have been formed by the action of eddies. The temperature difference of 4 m °C observed at a typical front requires a vertical downward displacement of approximately 50 m.

3.3.3. *Particle dispersion and residence time*

A tracer will be dispersed within the benthic boundary layer by three principal processes.

(a) *Vertical mixing*. Three-dimensional turbulence within the layer will mix a tracer over the depth of the layer. The mixing time, τ, is given by

$$\tau \approx h^2/4A_v, \tag{4}$$

where h is depth of the layer and A_v the vertical eddy diffusivity. Taking $h = 50$ m and $A_v = 50$ cm^2 s^{-1} then $\tau \approx 2$ d.

(b) *Tidal dispersion*. Tidal mixing will enhance the horizontal dispersion of a tracer through shear dispersion. An expression for the effective horizontal diffusion coefficient K_x, due to Bowden (1965), is

$$K_x \approx \alpha \bar{u} h, \tag{5}$$

where $\bar{u}$ is the depth-mean amplitude of the tidal velocity and α a constant of $O(1)$. Typical values for the deep ocean give $K_x \approx 10^3$ cm s^{-1}.

(c) *Eddy dispersion*. For periods in excess of a few days, the large length- and timescales of synoptic-scale eddies will dramatically increase the effective diffusion coefficient. An estimate of the diffusion coefficient is given by

$$K_x \approx T_l \bar{u}^2, \tag{6}$$

where $\bar{u}^2$ is now the variance of the eddying motions and T_l the lagrangian integral timescale. Again, for the deep ocean we expect (Saunders 1983)

$$K_x \approx 10^6\text{–}10^7 \text{ cm}^2 \text{ s}^{-1}.$$

Dispersion above and within the benthic boundary layer by synoptic-scale eddies was studied by seeding the flow given by the model of Richards (1984) with particles. The flow field taken was that of the experiment shown in figure 4. Arrays of 289 particles were released with an initial separation of 16 km both within the benthic boundary layer and the layer above. The model was then run on for a further 90 days and the tracks of the individual particles calculated. Five such releases were done giving a total of 1445 particle tracks in each layer. A measure of the spread of particles is given by the mean squared separation between particles $\langle R^2 \rangle$ taken over all particle pairs with an initial separation of 16 km. Once the mean separation between particles is larger than the integral length scale of the eddies then, because the turbulence is homogeneous and isotropic, the rate of change of $\langle R^2 \rangle$ becomes constant. The effective eddy diffusion coefficient is then given by $\frac{1}{4}\mathrm{d}/\mathrm{d}t\langle R^2 \rangle$. The diffusion coefficient above the layer was found to be $K_x = 8 \times 10^6$ cm^2 s^{-1} in good agreement with expression (6). Within the layer this value is reduced to $K_x = 5 \times 10^6$ cm^2 s^{-1}. (The layer diffusivity can be sensitive to the model parameters. Reducing the undisturbed mixed layer to 15 m gives a somewhat different flow régime with large areas of shallow mixed layer and a strong interaction between the mixed layer and the flow above. In this case the mixed layer diffusivity was found to be a factor of ten less than the diffusivity above the layer.)

In calculating the tracks of particles placed in the mixed layer it has been assumed that the particles remain in the layer. In practice some of these particles will escape from the boundary

when fluid is lost from the layer either through detachment of the layer from the bottom or by the ejection of fluid at fronts. The numerical model predicts likely places of mixed layer separation (§3.3.2). It is assumed that a particle entering such an area will escape from the bottom layer. After 90 days only 10% of particles not initially placed in a possible detachment site were lost. Extrapolating these results to later times gives an estimate of 800 days for the average residence time of particles in the mixed layer. As it is uncertain whether all warm patches will detach from the bottom this time should be treated as a lower bound on the residence time. The residence time for fluid in regions where the mixed layer is deeper and colder is therefore much greater than the average residence time for all particles, approximately 100 days. In 800 days, with a diffusivity of 5×10^6 cm s^{-1}, a tracer cloud initially 10 km in diameter will have increased to a diameter of 400 km with two-thirds of the tracer having escaped from the bottom.

3.4. *Topography*

In 800 days a fluid particle within the mixed layer is likely to have encountered an abyssal hill or the sides of a basin. It is therefore important to consider the effects of topography on the structure of the mixed layer and possible mechanisms for fluid escape. Topography can affect the near surface flow in two ways. Firstly, the flow will be distorted as it encounters the topography. This will tend to produce anti-cyclonic flow over hills and cyclonic flow over depressions (see, for example, Hogg 1980). Observations of anti-cyclonic flow over hills in the deep ocean include Gould *et al.* (1981) and Saunders (1988).

Secondly, the boundary layer may separate from the surface of the topography, a particularly effective mechanism for fluid to escape from the boundary. The topology of the separation depends strongly on the horizontal length scale of the hill, L, the hill height, h, the speed of the flow, U, and the stratification of the fluid, or buoyancy frequency, N. These can be combined to form the three non-dimensional parameters, the hill slope $\epsilon = h/L$, the Rossby number, $Ro = U/fL$, and the Froude number, $Fr = U/Nh$. A number of laboratory experiments have been conducted to investigate the dependency of the flow on these parameters, together with some theory. For small bell-shaped lumps, or hills, deep within the boundary ($h \ll \delta$) the effects of both the Earth's rotation and the weak stratification will be negligible ($Ro, Fr \gg 1$). The separation will be as sketched in figure 6*a* for a hill with moderate slope ($\epsilon \approx O(1)$, see Hunt & Snyder 1980). The flow in the lee of the hill is dominated by two counter-rotating, horizontal trailing vortices. The separation is open in the sense that a particle arbitrarily close to the surface upstream can be displaced permanently upwards into the body of the flow. As the horizontal scale of the hill increases such that Ro becomes $O(1)$ and $h \gg \delta$, the boundary layer depth, the structure of the separation changes to a single dominant trailing vortex (Richards *et al.* 1990). For situations in which either Ro or $Fr \ll 1$ (large horizontal length scales or strong stratifications) vertical motion is inhibited and the flow tends to be in horizontal

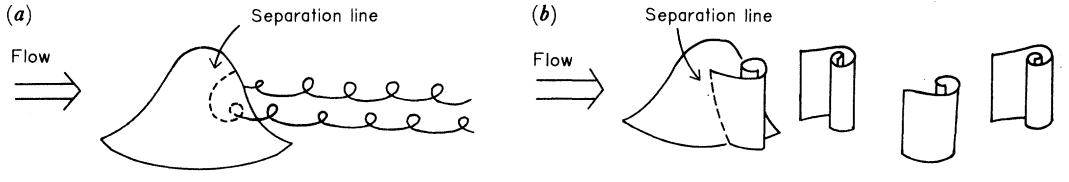

FIGURE 6. Schematic representation of the separated flow behind a bell-shaped hill for (*a*) homogeneous non-rotating flow ($R \gg 1$) and (*b*) rapidly rotating or strongly stratified flow ($R \ll 1$ or $Fr \ll 1$).

PHILOSOPHICAL TRANSACTIONS OF THE ROYAL SOCIETY A MATHEMATICAL, PHYSICAL & ENGINEERING SCIENCES

planes around the hill. Separation will now be in the form of eddies with vertical axes of rotation either attached, figure 2*d*, or shed, figure 6*b* (Boyer *et al.* 1987; Smeed 1990).

Figure 7*a* shows a number of temperature profiles in the lee of a hill on the Madeira abyssal plain obtained by yo-yoing a CTD. They show regions up to 2 km away from the hill where the temperature gradient is almost homogeneous in a series of layers, suggesting enhanced mixing in the lee of the hill. The surfaces of constant potential temperature (figure 7*b*), approximate isopycnal surfaces, show great changes in thickness along the section. The flow parameters are $\epsilon = 0.2$, $Ro = 0.08$ and $Fr = 0.14$. These are marginal for the formation of closed streamlines, a Taylor column, above the hill, but we would expect the flow to be constrained to be predominantly around rather than over the hill. The temperature profiles do not show the existence of an extensive trailing wake, although it must be stressed that the measurements are severely limited. More detailed studies of different flow régimes over topographic features are required.

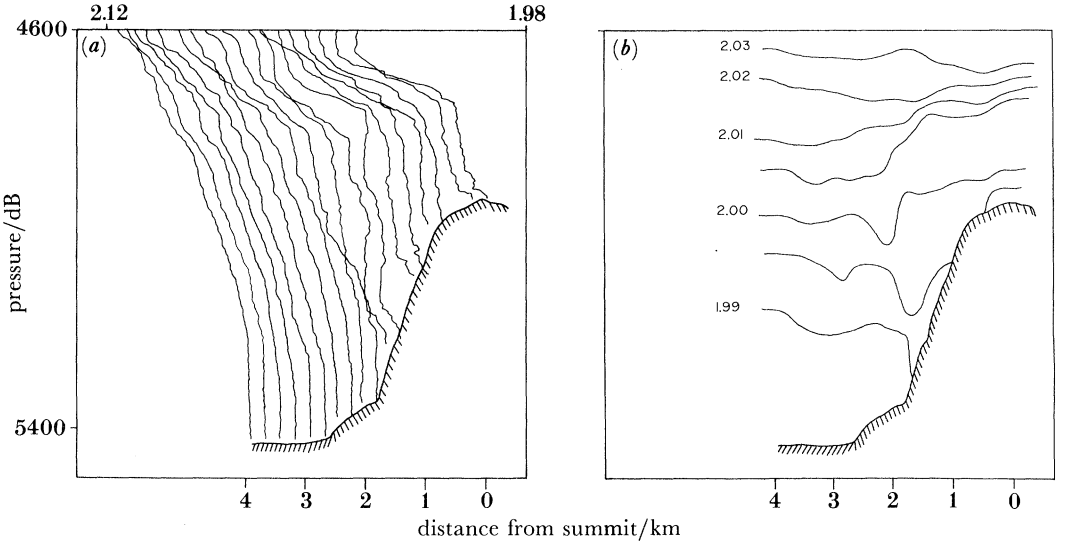

FIGURE 7. A number of potential temperature profiles, (*a*), and the potential temperature surfaces, (*b*), in the lee of a hill on the Madeira abyssal plain (courtesy of P. M. Saunders). Successive potential profiles are displaced by 5 m °C to the left. The flow is approaching the hill from the right of the figure. The hill height is 400 m and horizontal length scale 2.5 km. The flow speed is 2 cm s^{-1} and the buoyancy frequency $N = 3.5 \times 10^{-4}$ s^{-1}, giving $\epsilon = 0.2$, $Ro = 0.08$ and $Fr = 0.14$.

4. CONCLUSION

This paper highlights a number of physical processes that affect the density and current structure close to the sea-bed. To gain an understanding of bottom or near bottom processes we require to put mixing, chemical and biological processes into a proper physical context. This is also true in assessing the effect of ocean boundaries on interior processes; for instance it is still unclear where the majority of isopycnal mixing occurs in the ocean (the interior against edge question). For the bottom (including sloping regions) to be important, information needs to be transmitted to the interior. Simple Ekman pumping is not enough to transfer fluid and associated tracers. A number of boundary layer escape mechanisms have been identified although quantitative estimates for fluxes, etc., are still needed in many cases.

The richness in structure of the benthic boundary presents observational difficulties. Both theory and observations show that horizontal advection plays a dominant role. Individual point measurements are therefore usually difficult or impossible to interpret. Well planned tracer experiments may prove to be the answer. One such suitable tracer is ^{222}Rn which has a half life of four days. To date, measurements of this tracer have been rather haphazard although the study of Sarmiento *et al.* (1978) suggests the usefulness of this particular tracer. Sampling at time and space scales set by the physics of the processes discussed in §3 together with physical measurements will give a clearer picture of the mechanisms involved.

References

Armi, L. & D'Asaro, E. 1980 Flow of the benthic ocean. *J. geophys. Res.* **85**, 469–484.

Armi, L. & Millard, R. C. 1976 The bottom boundary layer of the deep ocean. *J. geophys. Res.* **81**, 4983–4990.

Bird, A. A., Weatherly, G. L. & Wimbush, M. 1982 A study of the bottom boundary layer over the eastward scarp of the Bermuda Rise. *J. geophys. Res.* **87**, 7941–7954.

Bowden, K. F. 1965 Horizontal mixing in the sea due to a shearing current. *J. Fluid Mech.* **21**, 83–95.

Boyer, D., Davies, P. A., Holland, W. R., Biolley, F. & Honji, H. 1987 Stratified rotating flow over and around isolated three-dimensional topography. *Phil. Trans. R. Soc. Lond.* A **322**, 213–241.

D'Asaro, E. 1982 Velocity structure of the benthic ocean. *J. phys. Oceanogr.* **12**, 313–322.

Elliott, A. J. *et al.* 1983 RRS *Discovery* Cruise 139: 12 July–3 August 1983. Bottom boundary mixing and the deep circulation in the east Atlantic. *Institute of Oceanographic Sciences*, cruise rep. no. 148 (22 pages).

Elliott, A. J. 1984 Measurements of the turbulence in an abyssal boundary layer. *J. phys. Oceanogr.* **14**, 1779–1786.

Gould, W. J., Hendry, R. & Huppert, H. E. 1981 An abyssal topographic experiment. *Deep Sea Res.* **28**, 409–440.

Hayes, S. P. 1979 Benthic current observations at Domes sites A, B and C in the tropical Pacific Ocean. In *Marine geology and oceanography of the Pacific manganese nodule basin* (ed. J. L. Bishott & D. Z. Piper), pp. 83–112. New York: Plenum Publishing.

Hogg, N. G. 1980 Effects of bottom topography on ocean currents. In *Orographic effects in planetary flows*. GARP publ. no. 23.

Hunt, J. C. R. & Synder, W. H. 1980 Experiments on stably and neutrally stratified flow over a model three-dimensional hill. *J. Fluid Mech.* **96**, 671–704.

McVean, M. K. & Woods, J. D. 1980 Redistribution of scalars during upper ocean frontogenesis: a numerical model. *Q. Jl R. met. Soc.* **106**, 293–311.

Richards, K. J. 1982*a* Modelling the benthic boundary layer. *J. phys. Oceanogr.* **12**, 428–439.

Richards, K. J. 1982*b* The effect of a bottom boundary layer on the stability of a baroclinic zonal current. *J. phys. Oceanogr.* **12**, 1493–1505.

Richards, K. J. 1984 The interaction between the bottom mixed layer and mesoscale motions in the ocean: a numerical study. *J. phys. Oceanogr.* **14**, 754–768.

Richards, K. J., Smeed, D. A., Hopfinger, E. J. & Chabert d'Hieres, G. 1990 Boundary layer separation of rotating flows past surface-mounted obstacles. (Submitted.)

Sarmiento, J. L., Broecker, W. S. & Biscaye, P. E. 1978 Excess bottom radon 222 distribution in deep ocean passages. *J. geophys. Res.* **83**, 5068–5076.

Saunders, P. M. 1983 Benthic observations on the Madeira abyssal plain: currents and dispersion. *J. phys. Oceanogr.* **13**, 1416–1429.

Saunders, P. M. 1988 Bottom currents near a small hill on the Madeira abyssal plain. *J. phys. Oceanogr.* **18**, 868–879.

Saunders, P. M. & Richards, K. J. 1985 Benthic boundary layer – IOS observational and modelling programme: Final Report, January 1985. *Institute of Oceanographic Sciences*. Rep. no. 199 (61 pages).

Smeed, D. A. 1987 A laboratory model of benthic fronts. *Deep Sea Res.* A **34**, 1431–1459.

Smeed, D. A. 1990 Separation of stratified rotating flow past three-dimensional topography. (Submitted.)

Thorpe, S. A. 1983 Benthic observations on the Madeira abyssal plain: fronts. *J. phys. Oceanogr.* **13**, 1430–1440.

Weatherly, G. L. & Kelly, E. A. 1985 Storms and flow reversals at the HEBBLE site. *Mar. Geol.* **66**, 205–218.

Weatherly, G. L. & Martin, P. J. 1978 On the structure and dynamics of the oceanic bottom boundary layer. *J. phys. Oceanogr.* **8**, 557–570.

Wimbush, M. & Munk, W. 1970 The benthic boundary layer. *The sea*, vol. 4, part 1, pp. 731–758. New York: John Wiley.

Woods, J. D., Wiley, R. L. & Briscoe, M. G. 1977 Vertical circulation at fronts in the upper ocean. In 'A voyage of Discovery', George Deacon 70th anniversary volume. *Deep Sea Res.* 253–275.

Wyngaard, J. C. 1975 Modelling the planetary boundary layer – extension to the stable case. *Bound.-Layer Met.* **9**, 441–460.

PHILOSOPHICAL TRANSACTIONS OF THE ROYAL SOCIETY A MATHEMATICAL, PHYSICAL & ENGINEERING SCIENCES